

UDC 621.10.56

DOI: 10.15587/1729-4061.2020.203279

*Представлені результати теоретико-експериментальних досліджень, направлених на установлення особливостей мікрорізання абразивними зернами, що характеризується активним виділенням шламу та пилових частинок. Частинки шламу частково видаляються із зони взаємодії, а частково змінюють поверхню інструменту та обробленої заготовки із вуглецевих композиційних матеріалів, зокрема, вуглець-вуглецевої та вуглець-полімерної груп.*

*Володіючи комплексом унікальних фізико-механічних властивостей, останні знаходять застосування у високотехнологічному виробництві, водночас композити все ще залишаються важко-оброблюваними матеріалами. Максимально проблеми виявляються при виконанні різних отворів, уступів, при вирізці вікон, обробленні крайок.*

*Дослідженням показано, що явище пило- та шламоутворення при абразивній обробці вуглецевих порожнистих композитів та пластиків уявляється наслідком ковзного руйнування та циклічного роззміщення поверхневого порожнистого шару, який виявляє квазікрихкі властивості під дією швидкорухомих мікроінденсторів. При цьому виявлена обумовленість середніх розмірів частинок шламу нормальними напруженнями в зоні різання та величиною виступання алмазних зерен над різальною поверхнею інструмента.*

*Оскільки встановлено, що частинки, які утворюються при різанні, лише частково видаляються за межі зони різання, і обсяг видалення зменшується зі зростанням часу обробки, зроблено висновок про причину зміни стану поверхні інструменту. Залишений шлам і бруд змінює топографію поверхні, внаслідок чого температура в зоні різання підвищується до критичних величин.*

*Показано, що використання інструментів із циклічною подачею дозволяє частково поліпшити умови обробки матеріалу, що є актуальним для реалізації процесів кільцевого алмазного свердлування, обробки алмазним полотном. Доведено, що зміна ділянок алмазозного шару зменшує явище налипання частинок бруду на поверхню робочого інструменту. Таким чином, інструмент довше залишається без забруднень і процес оброблення здійснюється ефективніше*

*Ключові слова: абразивне різання, свердлування, частота коливань, алмазне зерно, вуглецевий композиційний матеріал, шлам, пил*

# EFFECT OF SLIME AND DUST EMISSION ON MICRO-CUTTING WHEN PROCESSING CARBON-CARBON COMPOSITES

**A. Salenko**

Doctor of Technical Sciences, Professor  
Department of Machine Tools and Machinery Systems  
National Technical University of Ukraine «Igor Sikorsky  
Kyiv Polytechnic Institute»  
Peremohy ave., 37, Kyiv, Ukraine, 03056  
E-mail: salenko2006@ukr.net

**O. Chencheva**

PhD, Assistant\*  
E-mail: chenchevaolga@gmail.com

**V. Glukhova**

PhD, Associate Professor  
Department of Accounting and Finance\*\*  
E-mail: Glukhova710@gmail.com

**V. Shchetynin**

PhD, Professor\*  
E-mail: schetynin\_viktor@gmail.com

**Mohamed R. F. Budar**

Postgraduate Student\*  
E-mail: budar\_mohamed\_rf@protonmail.com

**S. Klimenko**

Doctor of Technical Sciences, Professor  
Department of Technological Control of Surface Quality  
V. Bakul Institute for Superhard Materials  
Avtozavodska str., 2, Kyiv, Ukraine, 04074  
E-mail: klimenko\_sa@protonmail.com

**E. Lashko**

PhD, Assistant\*  
E-mail: evgeny.lashko.lj@gmail.com  
\*Department of Industrial Engineering\*\*

\*\*Kremenчук Mykhailo Ostrohradskyi  
National University

Pershotravneva str., 20, Kremenchuk, Ukraine, 39600

Received date 23.02.2020

Accepted date 12.05.2020

Published date 19.06.2020

Copyright © 2020, A. Salenko, O. Chencheva,

V. Glukhova, V. Shchetynin, Mohamed R. F. Budar, S. Klimenko, E. Lashko

This is an open access article under the CC BY license (<http://creativecommons.org/licenses/by/4.0>)

## 1. Introduction

The use of new composite materials by machine-building complexes of the world's leading countries is constantly growing. This trend is due to the fact that the composites with a certain set of useful properties are prepared mainly

for the target products to maximally meet requirements for operating conditions or use in the future.

The composites possessing physical and mechanical properties such as strength, anisotropy, satisfactory heat resistance, low weight, high load carrying capacity, etc. required for high-tech production are hard-to-cut materials as yet.

Problems mainly become apparent in making various holes, shouldering, cutting windows, edging. The laboriousness of such operations exceeds material spreading out, impregnation with a binder and product formation taken together. This is primarily explained by the heterogeneous structure of composite materials. The substantial difference in mechanical properties of their components ultimately leads to a sharp deterioration in edge quality when trying to process such materials with common cutting tools. Phenomena of delamination, tear of reinforcing fibers, deterioration of edges result in a substantial rejection of finished products which ultimately brings about significant material losses. Scientists note that the problems can be bridged over in several ways, in particular, by using special tools [1] or applying a functionally-oriented approach in determining the sequence of processing operations [2], etc.

Workpieces from composites are quite often processed with abrasive tools. Because the material is a non-dense component medium, the process of micro-cutting with abrasive grains is characterized by active emission of slime and dust particles which are partially withdrawn from the zone of interaction and partially remain on the surface of the diamond layer. Also, the surface topography changes which leads to changes in the contact and sliding conditions in the cutting zone and, accordingly, to a sharp temperature rise and almost complete impossibility of processing in some cases.

Therefore, the establishment of patterns of slime and dust emission in processing composite carbon-carbon materials and the influence of the latter on the micro-cutting process is relevant and important for understanding the interaction of the abrasive layer of the working tool surface with loose anisotropic material. This will offer more effective ways and means to combat this phenomenon and increase the efficiency of processing carbon composites in general.

---

## 2. Literature review and problem statement

---

It was shown in [1] that fibrous composite materials (primarily polymers) have low machinability and the parts made of them can be mechanically cut only with special tools. These materials are prone to destruction, damage, and edge deterioration and a series of other defects that can lead to rejection of finished products.

Better processing (with a minimum number of defects) is possible only with special diamond-bearing tools [2]. The problem of chip formation during milling [2, 3] and subsequent overheating of the working tool remain unsolved because the working tool edges constantly change the cutting force vector in an anisotropic medium. The same applies to drilling [4, 5], especially when using tools with cutting inserts. Non-dense structure of the processed material reinforced with carbon fibers imposes additional restrictions on problem statement in determining rational processing conditions. Abrasive processing can significantly improve the quality of the surfaces formed during cutting but according to [6], it requires further studies of the accompanying phenomena causing surface defects in the top and bottom edges. Thus, even under these conditions, the emergence of various defects is quite likely.

The possibility of using diamond-based drills to make holes in parts of composite materials is shown in [7]. It is noted that the heterogeneous structure of materials and anisotropy of their properties require additional measures

to prevent the delamination of the processed materials and reduce the likelihood of defects.

The authors of [8] present results of their study of near-surface damages in workpieces of glass-fiber composite materials but the conditions for obtaining quality surfaces are not reported because the authors failed to generalize laws of tool action on anisotropic medium with pronounced plastic-elastic properties. The authors consider the medium dense (in contrast to non-dense carbon-carbon composites for which this feature is decisive).

Authors of [9] considered damages in a workpiece when the drill comes out of the hole during drilling linking them to conditions of tool loading. However, in principle, these studies did not differ from those discussed above because the material itself was a component medium with no cavities and had average physical and mechanical characteristics. Also, all studies solved the problem of interaction of the tool edges with the material in a quasi-stationary statement without taking into account the accompanying phenomena (in particular, the formation of chips or microchips, that is slime) and the changes in interaction conditions during the processing cycle.

All above-mentioned allows us to conclude that the processing of carbon-based composite materials is currently insufficiently studied. The lack of scientific basis for peculiarities of slime and dust emission in processing anisotropic non-dense materials necessitates studies of abrasive processing of composites taking into account the accompanying phenomena, in particular, slime and dust emission. This is also facilitated by active modification of these materials (such as KIMF) and their increasing use in engineering practice.

---

## 3. The aim and objectives of the study

---

The study objective implies the elaboration of ideas about abrasive processing of non-dense composite carbon materials based on the establishment of patterns of slime and dust emission with determining impact on the cutting process and a search for new, more efficient processing methods. To achieve this goal, the following tasks were set:

- to establish patterns of dust and slime emission in abrasive treatment of carbon-based composites (such as KIMF and plastics);
- to elucidate the influence of dust and slime emission on temperature change in the cutting zone;
- to elucidate the influence of the factor of using tools with cyclic advancement on conditions of material processing;
- to establish the influence of the effect of cyclically variable action of individual distinct sections of the diamond layer on dust emission and processing as a whole.

---

## 4. Materials and methods used in the study

---

The issues addressed in [10] were related to the simulation of the process of micro-cutting non-dense materials. Such materials often include carbon-carbon materials (Fig. 1, *a*), although reinforced plastics sometimes have substantial cavities (Fig. 1, *b*).

Description of the phenomena of dust and slime formation as a consequence of intermittent contact of working grains follows from the notion of a material as an aggregate of similar structural zones described based on the principal

structural element (PSE) of the composite. Let such an element be a body with diameter  $d_v$  having a matrix layer  $s_{pv}$  and a cavity layer  $s_{pp}$  on its surface (Fig. 2).

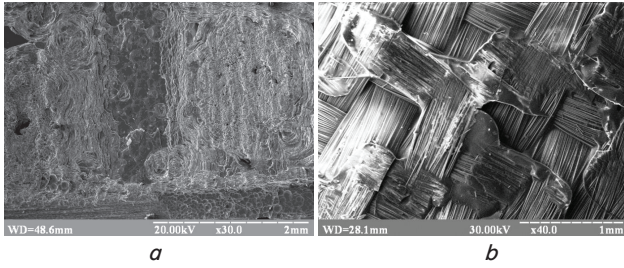


Fig. 1. Structure of the materials under study: *a* – KIMF carbon-carbon material; *b* – fiberglass

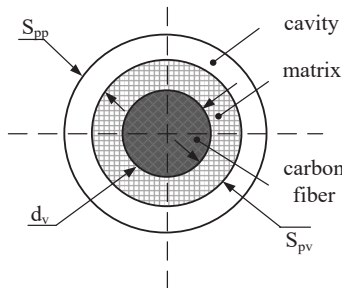


Fig. 2. The principal structural element

Depending on their location on the tool surface, the grains will act as cutting and contacting grains. The face surface which can be represented at a macro level as a discontinuous surface layer with a pitch of cavities  $t_p$  defined as  $t_p = d_v/2 + s_{pp} + s_{pv}$  takes a load from individual cutting grains. According to [11], such an interaction can be represented as an abrupt depression of a conical indenter under the action of the axial force  $P_z$  to a depth  $h$  resulting in a chip with a shearing angle  $\beta$  followed by applying a tangential force  $P_y$ . In the beginning, the indenter slides along the cone generatrix upwards under the action of the component  $t$  until the moment when the force  $P_z$  will be sufficient to destroy a layer to a depth  $h_1$ . The indenter overcomes friction forces between the chips and the base material. The amount of slip of the indenter is determined by the radius of the rounding of a single grain. Interaction of the diamond grain with the processed material surface at a ratio of indentation depth  $h$  to the radius  $\rho$  of the cutting edge rounding less than 0.01 is characterized by the elastic edging of the material, that is with no material removal.

Therefore, we can assume that the abrasive grain consistently interacts with the PSE components on its way.

Under the action of a normal force at the contact point, stresses are determined from corresponding Hertz formulas which for the case of contact of the abrasive grain with rounding  $r_1$  and radius  $r_2$  of the rigid component (a fiber bundle) according to the PSE notion will be as follows:

$$\sigma_k = \frac{m_p P_z^{1/3} E^{2/3}}{r^{2/3}},$$

where  $m = 1 + (r_1/r_2)$ ,  $E$  is the reduced modulus of elasticity:

$$E = \frac{2E_1E_2}{E_1 + E_2},$$

where  $r$  is the reduced contact radius:

$$\frac{1}{r} = \frac{1}{r_1} + \frac{1}{r_2}.$$

The contacting grains located mainly in the side surface interact with the surface due to elastic edging of the fiber bundles that have recovered after the action of the cutting grain.

Since the tensile strength of the fibers far exceeds the stresses created by the cutting grain, it can be assumed that the fibers that come to the surface and are connected to the matrix base will be destroyed by the mechanism of microcrack opening in the adhesion planes.

Destruction of the material structure and slime appearance take place both due to the sliding micro-cutting of the matrix (pyrocarbon) and the manifestation of the mechanisms of low-cycle softening followed by tearing off the reinforcement microfibers.

The frequency of loading of the surface elements determined by parameters of the cutting layer, the PSE structure, is:

$$\omega = \frac{\pi D}{\frac{d_v}{2} + s_{pp} + s_{pv}} n,$$

where  $D$  is the diameter of the tool used,  $n$  is rotation speed. The stress intensity factor will be:

$$k = \sigma_k + \left(\frac{b-l}{b}\right) \frac{3M_f}{2b^2} \cos \omega t \sqrt{\pi a},$$

where  $a$  is half the length of the open crack,  $M_0$  is the moment of perturbation,  $b$  and  $l$  are geometric parameters of the microcrack.

Based on the patterns of release of elastic deformations according to [9] and the data of [10], the expected maximum crack length  $a_c$  after a certain cycle of loads  $N$  will be as follows:

$$a_c = \frac{a_0}{\sqrt[n/2-1]{1 - \frac{\pi CDnt}{\left(\frac{d_v}{2} + s_{pp} + s_{pv}\right) K}}}, \tag{1}$$

where

$$C = a_0^{n/2-1} \left(\frac{\sigma}{\rho}\right)^n \left(\frac{\rho}{\bar{c}}\right)^n,$$

$$K = \frac{1}{\sqrt{\pi(n/2-1)}},$$

$a_0$  is the initial crack length;  $\rho$  is the density of the material;  $n, \bar{c}$  are material constants;  $\sigma$  is microstress at the crack tip. A particle of material (fiber bundle, pyrocarbon matrix) is separated when critical stresses or strength of the composite component are exceeded and the expected size of such a particle is  $a_c$ , that is  $d_p - a_c$ .

Particles formed during cutting (in the amount of  $I_u$ ) will be withdrawn from the cutting zone ( $I_l$ ) and partially deposited on the surface of the cutting edges ( $I_o$ ):  $I_u = I_l + I_o$ . In this case, their total volume will be  $W_s$  and distribution between

withdrawal from the cutting zone  $W_p$ , getting into the material cavities  $W_r$  and on the tool surface in the intergranular cavity  $W_i$  will correspond to:

$$W_s = W_p + W_r + W_i. \quad (2)$$

The amount  $I_u$  is determined by the material structure, topography of the diamond layer, and the processing modes.

Regularities of removal of particles from the cutting zone are determined by the movement of the working surfaces of the tool (rotational and reciprocal), the geometry of the working section and the working gap. The particles of material left on the contact surfaces after cutting will bring about an increase in the contact area, contact stresses, and temperature in the cutting zone.

The higher the temperature, the more actively the particles will stick to the surface with the creation of a strong sintered layer. The reason consists in the fact that the pyrocarbon of the matrix (especially low-temperature pyrocarbon obtained at pyrolysis temperatures around 800 °C) is actively destroyed under the action of high temperatures with the formation of individual fragments, disperses and penetrates the tool surface cavities under the action of pressure. Therefore, temperature  $T$  on the working surfaces of the tool is another factor influencing the removal of particles from the cutting zone.

To consider the equilibrium of the particles formed in the cutting zone, it is advisable to consider the forces acting on the particles at the face and in the peripheral zone (Fig. 3).

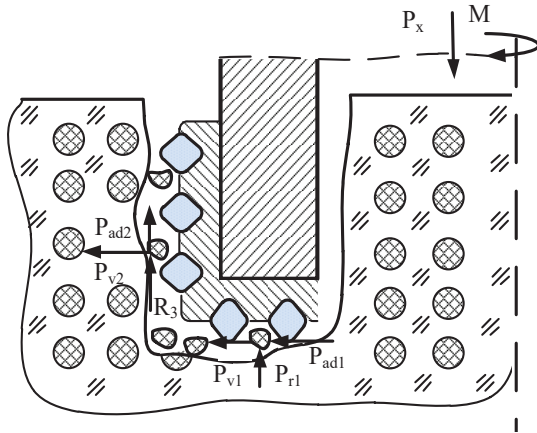


Fig. 3. Forces acting on particles at the face and in the peripheral zone

The following forces act on the separated particles of slime and dust in the interfacial gap:

$$\vec{F} = \vec{P} + \vec{F}_a + \vec{F}_v + \vec{F}_z + \vec{F}_f + \vec{F}_k,$$

where  $P$  is the attractive force;  $F_a$  is the aerodynamic force;  $F_v$  is the centrifugal force;  $F_z$  is the adhesion strength,  $H$ ;  $F_f$  is the force of friction of the particle on the surface;  $F_k$  is the force of contact interaction. In the first approximation, the aerodynamic force  $F_a$  is represented as a force of airflow in the gap taking into account non-uniformity of its velocity in the near-surface zone, therefore, taking into account [10], it can be defined as follows:

$$F_a = \rho c S \frac{u^2}{2} + \rho_c \frac{\pi r^3}{2} u \frac{du}{dz},$$

where  $c$  is the drag coefficient of the slime particle;  $\rho$  is the air density;  $\rho_c$  is the density of the particle material;  $r$  is the particle radius;  $S$  is the cross-sectional area of the particle;  $u$ ,  $du/dz$  are the average velocity of the airflow and its gradient along the  $z$  axis.

Particles can interact to form individual conglomerates or stick to the surface due to the phenomenon of adhesion. The adhesion strength is:

$$F_z = 2.4 \cdot 10^{-7} r,$$

where  $r$  is the particle radius.

The centrifugal force is defined as  $F_v = m\omega^2 R_i$ , where  $R_i$  is the radius of the particle path;  $\omega$  is the angular velocity;  $m$  is the particle mass; the friction force between the particle and the plane is  $F_f = \mu F_k$ .

The forces of contact interaction will be determined on the condition that after their separation, the particles have a certain velocity vector directed along the tangent to the radius of the particle location near the grain.

Let the tool, in addition to rotational, perform reciprocating cyclic motion.

According to the law of momentum conservation and proceeding from the condition that the contact between the abrasive particle and the slime particle lasts  $t$  s, we have:

$$F_u = \frac{mv}{t},$$

where  $t = A/v_v$ ,  $A$  is the amplitude of the tool oscillations in the vertical plane;  $v_v$  is the velocity of vertical movement of the tool. Then, assigning the forces to the corresponding coordinate axes, we can make differential equations of the behavior of individual particles in the facial and peripheral gaps.

In accordance with the d'Alembert principle, differential equations of equilibrium of particles in projections on the  $r$  and  $z$  axes will take the form:

$$\begin{aligned} m_p \frac{d^2 r}{dt^2} &= \sum F_{ri}, \\ m_p \frac{d^2 z}{dt^2} &= \sum F_{zi}. \end{aligned} \quad (3)$$

when a slime particle is moving in the gap between the tool face and the cutting surface in the horizontal plane, a centrifugal force and a force of contact interaction, friction, and adhesion forces act on it. The forces of the aerodynamic load can be neglected.

The system of forces acting on a particle in the peripheral gap will include the aerodynamic component, friction force, contact interaction force, adhesion, and the particle weight. The conditions for the movement of particles are as follows. For the facial gap: movement along the  $OR$  axis:  $F_v - F_a - F_f - F_z > 0$ ; the condition for withdrawal of particles from the peripheral gap along the  $OZ$  axis will take the following form:  $F_u - F_v - F_a - F_f - mg - F_z > 0$ .

In the first approximation, movement of air in the gap during the reciprocal movement of the tool is obtained from the Quetta flow, that is:

$$\frac{\mu d^2 u_r}{dz^2} - c_1 = 0.$$



Thus, we have the following system of equations:

$$\begin{aligned} \frac{4}{3}\pi r^3 \rho \frac{d^2 r}{dt^2} &= m\omega^2 R_i - 2.4 \cdot 10^{-7} r - \\ &- \mu_p mg - \left( \rho c S \frac{u_z^2}{2} + \rho_c \frac{\pi r^3}{2} u_z \frac{du_z}{dz} \right); \\ \frac{4}{3}\pi r^3 \rho \frac{d^2 z}{dt^2} &= \frac{mv(\cos(\omega t))}{t} - m\omega^2 R_i - \\ &- 2.4 \cdot 10^{-7} r - mg - \left( \rho c S \frac{u_r^2}{2} + \rho_c \frac{\pi r^3}{2} u_r \frac{du_r}{dz} \right); \\ \frac{\mu d^2 u_r}{dz^2} - c_1 &= 0. \end{aligned} \tag{4}$$

To determine temperature  $T$  in the cutting zone, it is necessary to consider heat release on the contact surfaces. When moving in the material body, the grain performs the work of destruction at the contact length  $l_p$ . At the same time, due to restoration of the cut layer, the tool is contacting with the workpiece periphery and faces which makes it possible to determine heat balance as follows:

$$Q_p + Q_{tr} + Q_{dl} = Q_k + Q_i + Q_a, \tag{5}$$

where  $Q_p$  is the heat release at the tool periphery;  $Q_{tr}$ ,  $Q_{dl}$  are the heat release at the right and left faces, respectively;  $Q_k$  is the heat absorption to the material;  $Q_i$  is the heat absorption to the tool;  $Q_a$  is the heat loss to environment and slime.

Assume that the work of external forces in the cutting zone is divided into the work of destruction and the work of friction. If we take into account that the latter is completely converted into heat, then based on [7], the intensity of heat release will be:

$$q = fpv, \tag{6}$$

where  $f$  is the coefficient of friction ( $f=0.18$  for carbon under the condition of linearization at high speeds);  $p$  is the contact pressure;  $v$  is the sliding velocity.

The authors of [12] note that the contact pressure is determined by the ratio of the force of normal load  $F$  to the contact area  $s_k$ . Under the action of the normal force at the point of contact, stresses can be determined by appropriate Hertz formulas which for the case of contact of an abrasive grain (represented as a sphere of radius  $r_1$ ) and a bundle of fibers of radius  $r_2$  will be:

$$\sigma = \frac{mF^{1/3} E^{2/3}}{r^{2/3}},$$

where

$$m = 1 + \frac{r_1}{r_2},$$

$E$  is the reduced modulus of elasticity:

$$E = \frac{2E_1 E_2}{E_1 + E_2},$$

$r$  is the reduced contact radius:

$$\frac{1}{r} = \frac{1}{r_1} + \frac{1}{r_2}.$$

Since contact of grains is nonconstant during the processing of the composite material with a porous structure, the contact time (and, accordingly, the heat release intensity) will be determined by the density of the composite reinforcement weaving, density of the abrasive-containing (diamonds) layer and velocity of relative motion.

For geometric reasons and provided that a part of the fiber is cut only when the fiber protrudes above the surface by an amount of  $\psi$ , maximum contact length will be:

$$l_k = 2\sqrt{r_2^2 - (r_2 - \psi)^2}.$$

Simultaneously,  $N$  contacts will take place in the processing area, so the reduced contact length will be  $l_p = Nl_k$ , m. Then the time of contact interaction that will determine heat emission will be:

$$\tau = \frac{2N\sqrt{r_2^2 - (r_2 - \psi)^2}}{\pi D_k n}.$$

Frequency of occurrence of heat-emitting zones will be determined by the ratio:

$$\phi = \frac{\pi D_k n}{l_k}. \tag{7}$$

Small heat emitting zones receive heat from the contact interaction (Fig. 4). The problem of determining the distribution of temperature fields for them is reduced to the problem of pulsed heating of the surface by a point source. The determination of temperature on the heating surface is considered in [13].

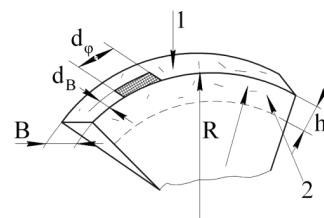


Fig. 4. Diagram of calculation of heat removal into the tool

The differential equation of thermal conductivity in a stationary medium which does not involve convection or radiation takes the form:

$$\frac{\partial^2 T}{\partial x^2} + \frac{\partial^2 T}{\partial y^2} + \frac{\partial^2 T}{\partial z^2} + q = \frac{1}{\rho C} \frac{\partial T}{\partial t}. \tag{8}$$

That is, we have the following temperature change for a particular body:

$$\begin{aligned} dT(x, y, z, t) &= \frac{\delta q}{\rho C (4\pi\alpha(t-t'))^{3/2}} \times \\ &\times \exp\left[-\frac{(x-x')^2 + (y-y')^2 + (z-z')^2}{4\alpha(t-t')}\right] \end{aligned}$$

for a point with coordinates  $(x, y, z)$  for time  $t$  if heat  $\delta q$  instantly reaches a point on the surface having coordinates  $(x', y', z')$  and time  $t'$ ;  $C$  is the heat capacity,  $\alpha$  is diffusivity,  $\rho$  is density,  $K$  is thermal conductivity.

Temperature change in a semi-finite body will occur in a somewhat different way:

$$\begin{aligned} dT(x, y, z, t) &= \\ &= \frac{\delta q}{\rho C (4\pi\alpha(t-t'))^{3/2}} \exp\left[-\frac{(x-x')^2 + (y-y')^2}{4\alpha(t-t')}\right] \times \\ &\times \left[ \exp\left[-\frac{(z-z')^2}{4\alpha(t-t')}\right] + \exp\left[-\frac{(z+z')^2}{4\alpha(t-t')}\right] \right], \end{aligned}$$

if heat is released at a rate  $dQ = Pd t'$  from  $t=t'$ ; to  $t=t'+dt'$  at the point  $(x', y', z')$ , the temperature at  $(x, y, z)$  at a time moment  $t$  is found by integrating the previous equation:

$$\begin{aligned} dT(x, y, z, t) &= \frac{Pd t'}{\rho C (4\pi\alpha(t-t'))^{3/2}} \times \\ &\times \exp\left[-\frac{(x-x')^2 + (y-y')^2 + (z-z')^2}{4\alpha(t-t')}\right]. \end{aligned}$$

Now, if the heat source from time  $t'=0$  to  $t'=t$  is continuous, it can be written as:

$$\begin{aligned} dT(x, y, z, t) &= \\ &= \int_{t'=0}^{t'=t} \frac{Pd t'}{\rho C (4\pi\alpha(t-t'))^{3/2}} \exp\left[-\frac{(x-x')^2 + (y-y')^2 + (z-z')^2}{4\alpha(t-t')}\right], \end{aligned}$$

where  $Q$  in  $W$ .

When  $t \rightarrow \infty$ , there will be a stationary temperature distribution given by the formula:

$$T(x, y, z) = \frac{P}{4\pi k \sqrt{(x-x')^2 + (y-y')^2 + (z-z')^2}}.$$

This temperature distribution is characteristic of the pulsed action of a heat source.

The equation that describes a one-dimensional temperature field relative to the tool periphery obtained on the basis of the solution to the differential equation:

$$q = q_0 A = -\lambda_T \frac{\partial T}{\partial x}(0, t)$$

is as follows:

$$T(x, t) = \frac{2q\sqrt{\alpha_T t}}{\lambda_T} i\Phi\left(\frac{x}{2\sqrt{\alpha_T t}}\right). \quad (9)$$

After cessation of the pulse of the heat source of duration  $t$  on the heated surface, it cools down due to redistribution of the heat input. Provided that the processed body is a semi-infinite space, one-dimensional temperature field can be found as follows:

$$\begin{aligned} T(z, t) &= \frac{2Aq_0\sqrt{\alpha_T}}{\lambda_T} \times \\ &\times \left[ \sqrt{t} i\Phi\left(\frac{x}{2\sqrt{\alpha_T t}}\right) - \sqrt{t-\tau} i\Phi\left(\frac{x}{2\sqrt{\alpha_T(t-\tau)}}\right) \right]. \quad (10) \end{aligned}$$

Surface temperature will be:

$$T_0(t) = \frac{2q\sqrt{\alpha_T t}}{\lambda_T}.$$

Therefore, taking into account the pattern of temperature rise and changes in the activity of slime particles relative to the tool surface, equation (2) will take the form:

$$W_s = W_p + W_r + W_i(T). \quad (11)$$

If processing is performed with a cylindrical tool having diameter  $D_s$  with a flat face perpendicular to the cylinder axis for which density of diamond grains  $\eta$  on the tool surface is such that together they cut a material layer when the cylinder turns at an angle  $\alpha$ , the theoretical volume  $W_s$  of the withdrawn material will be:

$$W_s = f(t) = \left[ \frac{R_1^2(\alpha - \sin(\alpha))}{4} + vt \right] l \vartheta. \quad (12)$$

where  $\vartheta$  is the density of the material (assuming that the processed medium is non-dense).

Thus, to determine  $W_s$ , we use equation (11), and to determine  $W_p$ , we use the system of equations (4) and the equation of temperature limits (10). Because particles are in a cavity between the surface of the cutting tool and the cutting plane, the concentration of particles as a ratio of their quantity to the cavity volume is an important characteristic. For a rotating and reciprocating tool, this volume will be determined as follows. The tool will make  $M$  double strokes with amplitude  $A$  during time  $\tau$  of turning by a  $2\pi$  angle. Then a gap is formed between the facial surfaces. Its volume can be defined as follows:

$$W_t = \left[ \frac{\pi(D_z^2 - D_v^2)}{4} \left( l_p + \frac{A}{2} \right) - \eta \frac{4\pi r_a^3}{9} \right] \sin \omega \tau,$$

and

$$W_b = \left[ \pi D_z AM(l_p) - \eta \frac{4\pi r_a^3}{9} \right] \sin \omega \tau$$

on the periphery.

If the slime particles are considered as balls with radii  $r_s$ , their volume concentration, taking into account the frequency of grain contacts (7) with the surface resulting in the appearance of slime particles, will be:

$$K_i = \frac{\left[ \frac{\pi(D_z - D_v)n}{l_k} \right] w_s \tau - W_r - W_i(T)}{4 \left[ \frac{\pi(D_z^2 - D_v^2)}{4} \left( l_p + \frac{A}{2} \right) - \eta \frac{4\pi r_a^3}{9} \right] \sin \omega \tau + \left[ \pi D_z AM(l_p) - \eta \frac{4\pi r_a^3}{9} \right] \sin \omega \tau}. \quad (13)$$

where  $D_z$ ,  $D_v$  are the outer and inner diameters of the tool, respectively;  $n$  is the speed of tool rotation;  $\tau$  is the current time;  $w_c$  is a particle volume.

An increase in this parameter will lead to an increase in temperature in the cutting zone and a decrease in the process productivity.

To check theoretical premises regarding the influence of the contact zone parameters on efficiency and quality of the obtained surface layer when processing materials such as KIMF (its properties are given in Table 1) with a diamond tool and setting the thermal regime, FDB Maschinen GYQ400B/220 machine tool was used.

Table 1

Mechanical properties of CFRC, KIMF type

Volume (imaginary) density, g/cm <sup>3</sup> , not less than	1.7 g/cm <sup>3</sup> (actually not less than 1.78 g/cm <sup>3</sup> )
Fracture stress for compression in reinforcement axes X(Y), kg/cm <sup>3</sup> , not less than	1.200 (actually not less than 1.700)
Fracture stress for tension in reinforcement axes X(Y), kg/cm <sup>3</sup> , not less than	240 (actually not less than 600)
Shear fracture stress, MPa, not less than	24.5
Bending fracture stress, MPa, not less than	88.2
Heat conductivity coefficient (at 50 °C), kcal/m h, deg.	7
Modulus of elasticity for compression in reinforcement axes X(Y), MPa, not less than	2.45·10 <sup>4</sup>
Material porosity, %	×8.7
Impact strength, kJ/m <sup>3</sup>	×10
Electrical resistivity, Ohm·mm <sup>2</sup> /m	30

Processing was performed with an 18.0 mm dia. diamond ring drill (Table 2). The study of the surface layer and the resulting slime was performed with REM-106-I scanning electron microscope. Samples were prepared from carbon-carbon materials of regular weaving. Cutting was carried out in the modes recommended by the manufacturer of tools for stone processing. The temperature in the cutting zone was measured with Maurer Digital Infrared Pyrometer, Series KTRD 1065. The study results were processed using special Maurer IR-LOG software. Cutting forces in the contact zone were measured using ZEMIC BM3-C3-0.2-3V strain-gauge transducer connected to M-DAQ ADC having a resolution of 2.0 N with recording to a computer file.

The effect of the degree of contamination of the tool surface layer was determined by weighing the samples with precision RADWAG type scales having a division value of 0.0001 g and a weight limit of up to 150.000 g.

It was taken into account that when the amount of the substance is  $W_i^{\max}$ :

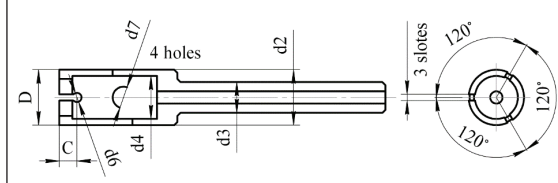

$$W_i^{\max} = 3\pi D_k h \delta - \frac{2}{3} \pi r_a^3 N,$$

where  $N$  is the number of abrasive grains;  $r_a$  is the radius of the abrasive grain, which is conventionally considered a hemisphere, the circle contact will correspond to the disk contact with a surface in the absence of destruction work.

The study of dispersity and type of the slime obtained by abrasive cutting was performed by scanning micro electron microscopy.

Table 2

Medium diameter drills used in the study

No.	Drills and their parameters
1	<p>Ring drill</p>  <p><math>D=14-24</math> mm; <math>c</math>: hole depth; <math>d6</math>; <math>b</math>: width; <math>d2</math>, <math>d3</math>, <math>d4</math>, <math>d7</math>: dimensions of constructs. Grain size: 160/125 Drilling 14.0 to 24.0 mm dia. holes</p>
2	 <p>18.0 mm dia.drill; diamond layer with regular stress-relief strips Drilling 18.0 mm dia. holes in carbon-based materials</p>

For this purpose, chemicals were prepared after processing workpieces for the microelectronic study of both the obtained surfaces and the slime material (microchips) after processing. The samples were glued to a conductive foil and kept at +85 °C in a VUP-5 vacuum chamber in a low vacuum (1.0–2.0 Pa) for 12 h. After that, the samples were placed on a microscope stage providing a reliable electrical contact for the removal of electronic potential from the stage. To assess the influence of the  $S_p$  parameter on the process of slime removal, a microelectronic study of the surface of the cutting tool, that is an 18.0 mm dia. tubular drill, was performed. To determine the magnitude of grain protrusion, a TL-90 type profilometer was used.

## 5. Results of experimental and model studies of the process of diamond micro-cutting of carbon-carbon composites

### 5.1. Dust and slime emission during abrasive processing of carbon-based composites (of KIMF type) and plastics

Examination of the cutting tool surface (diamond layer) has proved (Fig. 5, a) that diamond grains protruded above the surface to a height of 0.02–0.18 mm. The average value was 0.12 mm and the dispersion of the grain top protrusions above the surface obeyed, in general, the law of normal dispersion. Individual diamond grains in a fraction of 150–200 μm were observed on the surface of the cutting tool edges (Fig. 5, b). The density of such grains was 250–300 pcs/cm<sup>2</sup>. The diamond layer was not smooth which can be explained by peculiarities of the technology of fixing diamonds to the surface.

To study dispersity and average particle size and model the slime withdrawal processes, we used raster processing software and automatic generation of an area with a corresponding contrast. This has allowed us to determine slime particle size by micro- and microelectronic photography of samples. Then, the number of closed contours will correspond to the number of particles, and the fields differing by their brightness will show the presence of a particle or

a substrate. The existence of several concentric contours (for example, if the test particle has surface cavities, protrusions, etc.) is leveled-off by the introduction of appropriate correctors and image masks. A single layer of particles for the study is the condition for the calculation accuracy.

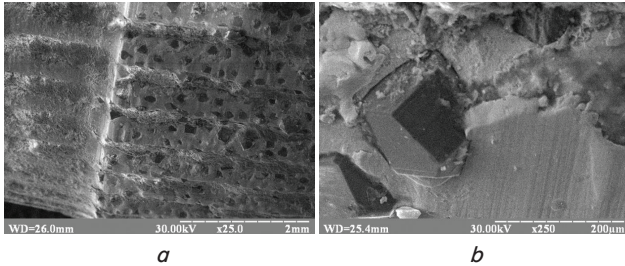


Fig. 5. Microelectronic photographs of the surface of a diamond-based tubular drill: *a* –  $\times 25$ ; *b* –  $\times 250$

This has allowed us to establish geometric parameters of the PSE taken into account (Fig. 2). For example, the carbon fiber bundle represented by the PSE core had diameter  $d_v=1.57-1.72$  mm; the polymer matrix covered the bundle with a layer of  $s_{pp}=0.35-0.55$  mm; thickness of the intermediate layer with air cavities was  $s_{pv}=0.18-0.22$  mm.

Analysis of electron micrographs proved the quasi-brittle nature of fracture of the composite components and isolated particles of the polymer matrix, fragments of broken fibers and conglomerates in which cracks have grown to a critical size. Comparison of slimes in terms of fractional composition has proved that the slime of the side surfaces (Fig. 6, *a*) was fine, homogeneous, with an average particle size of 40–80  $\mu\text{m}$ ; the slime from the face part of the drill was coarser (Fig. 6, *b*): its fraction was 120–160  $\mu\text{m}$ . At the same time, the slime contained separate fractions of cut carbon fibers and the matrix. Therefore, we can conclude that the particles moving in the surface gaps undergo significant changes in shape and their fining occurs resulting in an increase in the number of fine components.

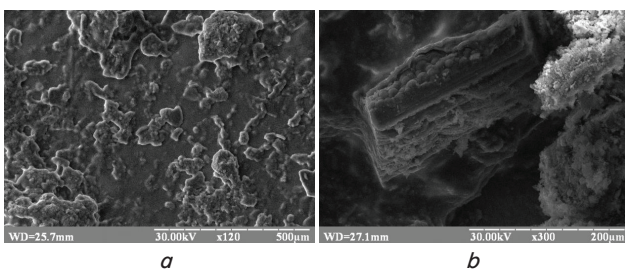


Fig. 6. Microelectronic photographs of slime in the cutting zone: *a* – slime from the side surface; *b* – slime from the tool face

It was proved that the characteristic particle size (for example, length  $l_z$  or larger size) is determined by:

- 1) orientation of the reinforcing fibers relative to the applied force;
- 2) dimensions of the protruding parts of abrasive grains;
- 3) stresses in the surface layer  $\sigma_0$  due to the axial advancement force  $P$ .

Force action on the treated material has the most significant influence on the slime particle size (Fig. 7, *a*). This causes the emergence of stresses in the surface layer  $\sigma_p$ .

It can be expected that an increase in the applied axial force will cause a corresponding increase in stresses on the contact surface and spall individual fibers and their conglomerates. It is seen from the given diagram that the excess of stresses over 40 MPa significantly increased the slime particle size. Based on the physical model of surface formation by an individual grain, it can be concluded that the surface roughness will increase. These results are reflected in [10].

The effect of fiber orientation on the slime fractionation was insignificant within the stress range of 15–40 MPa, orientation of the fibers at angles approaching  $\pi/4$  results in a 20–35 % decrease in the slime fractionality.

Size of the console of the protruding part of the diamond grain almost linearly changed the expected fractionality of the slime (Fig. 7, *b*): reduction of the protrusion to 0.08 mm changed microstresses at the top and affected the development of microcrack grids. Cracks began to grow more actively with the formation of particles 0.08–0.12 mm in size.

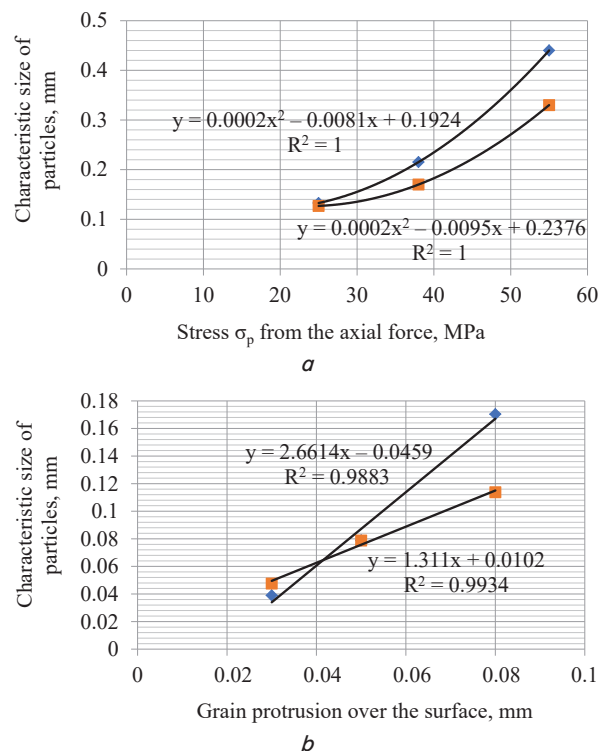


Fig. 7. Conditionality of particle sizes: by stresses from the action of the load oriented along the normal to the surface (*a*); by protruding part of abrasive grains (*b*)

Thus, it becomes clear that the presence of cavities in the material plays an important role in the process of its destruction by abrasive particles. For example, an increase in the force applied to the tool causes greater local deformation of the areas adjacent to the cavity. As a result, the fibers begin to separate from the matrix with the subsequent weakening of the entire near-cavity space.

Active crack formation on the planes of adhesion is the consequence of such weakening. This somewhat changes taking the force load by the material components: now we are talking about the fact that the fibers are excluded from the matrix, therefore, they are destroyed by fractures at a greater length. The matrix, in this case, is no longer a strong connector.



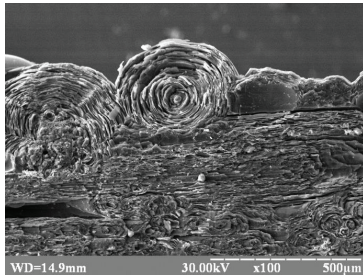


Fig. 8. A fragment of the near-cavity area with an emerged microcrack

**5.2. Temperature change in the cutting zone during active slime formation**

The analysis was performed for a case of processing with ring drills of conventional design (with a uniform application of a diamond layer on the cutting surface) and for the case of processing with drills having a profiled layer (Fig. 9).

Temperature fields were simulated for the case of the tool contact with the workpiece based on the following [14]:

- the drill material was homogeneous, with a single-layer application of diamonds by methods of electroplating or laser deformative sintering;
- the workpiece was in contact with the tool in points of contact with diamonds but the contact area depended on the intensity of slime formation due to the micro-cutting process;
- the slime firmly adhered to the base; the contact conditions did not change during the simulation.

The temperature increase was estimated from (10) with a time-discrete  $t=0.5$  s, provided that  $z=0.1$  mm. The results are shown in Fig. 10.

It becomes clear from the patterns of temperature distribution that with an increase in time over 2–2.5 s temperature on the contact surface begins to reach critical values (over 600–700 °C) and, consequently, growth of contact spots will be progressive.

The increase in temperature changes the dust fractionality. For example, Fig. 11 shows examples of formed slime conglomerates that become compacted with increasing temperature.

Therefore, it can be concluded that the temperature growth leads to the formation of conglomerated slime particles whose dimensions can significantly exceed the expected and theoretically calculated dimensions. At the same time, the number of small particles formed in a progressive number, in general, corresponded to the calculations by equation (13).

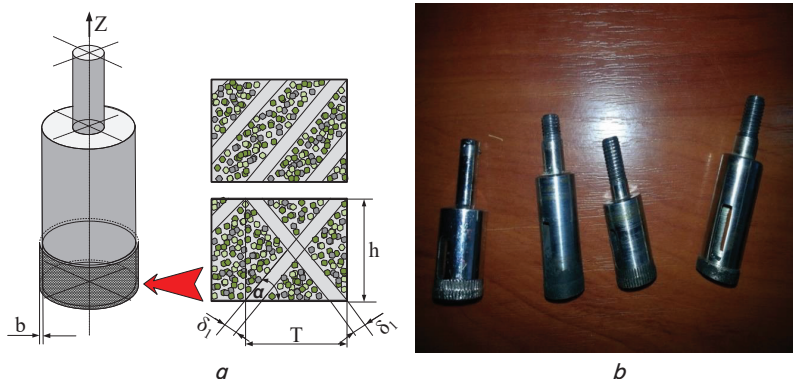


Fig. 9. The drills used in the study: a – schematic view; b – physical appearance

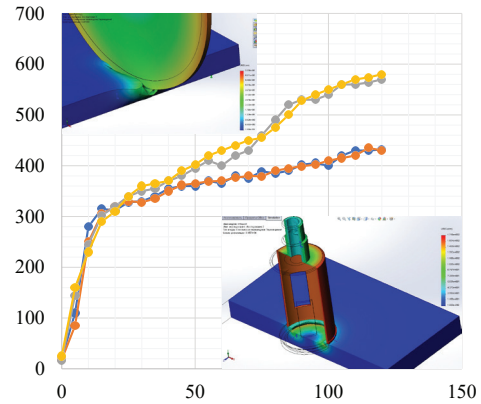


Fig. 10. Increase in temperature in the surface layer over time during processing with various abrasive tools

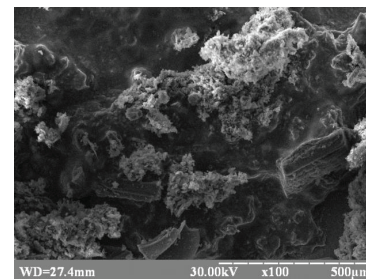


Fig. 11. Particles and conglomerates of fibers from the binder residues

**5.3. Influence of the factor of cyclic tool loading on the phenomena**

Typically, additional effects on tools such as axial load on drills, a normal load of the renovator saws, spindle of the abrasive wheel, etc. are used to increase machining efficiency. We have found that the oscillation frequency of the working tool directly determines slime dispersion.

For example, the vibration of the working body face in a frequency range 40–600 Hz should lead to the emergence of exclusively fine slime because from (1) cracks cease to develop and bifurcate with the formation of fine particles.

However, experimental studies have shown that the use of low-frequency load on the edges of the working body (in the frequency range 20–50 Hz) causes the appearance of quite significant slime particles whose characteristic size can be expected at a level of 0.18–0.27 mm. Since frequency has the opposite effect and the fiber bundles can be significantly loosened without a matrix, such particles can be formed mainly from the binder. Therefore, we know that the increase in the frequency of vibration of the working tool surface on the normal to the treated surface leads to a decrease in the slime particle size (Fig. 12).

The obtained results were taken into account and (13) curves of slime withdrawal from the cutting zone were constructed according to equations (4), depending on:

- the working load amplitude  $A_p$  and frequency  $H_p$ ;
- interfacial gap  $l_p$  determined by the protrusion of grains above the surface and the material hollowness;
- the density of the application of diamond grains on the tool surface,  $S_p$ .

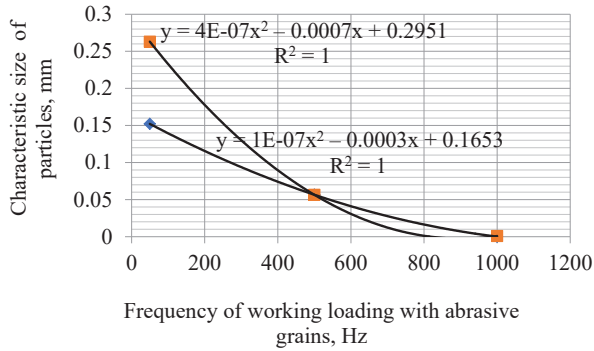


Fig. 12. Change of expected sizes of slime particles depending on the frequency of working loading by abrasive grains

The results of the simulation of the particle removal dynamics taking into account the reciprocal motion of the tool are presented in Fig. 13.

The calculation was performed up to a complete cessation of particle removal according to (11), that is when particles fill the cavity of the interfacial gap as much as possible.  $K_1$  corresponds to a cyclic frequency of 50 Hz,  $K_2 = 50$  Hz.

The change in concentration was established from equations (11), (13). As follows from the simulation results, the most efficient removal of particles is observed when the tool oscillates with a low frequency (within 30–50 Hz) with an amplitude of oscillations up to 1–2 mm. It can be seen from the above diagrams that the emission of slime particles is not constant. Over time, the specific indicators of slime production are expected to decrease (Fig. 13, a) while the concentration of slime particles formed during processing grows faster (Fig. 13, b).

It is also obvious that upon reaching a concentration of particles in the gap between the surface of the tool and the surface of the procession to a certain level, the phenomenon of slime conglomeration and its active adhesion to the surface will be observed.

Therefore, processing should be carried out so that the slime substance is completely withdrawn from the cutting area and does not create preconditions for changing the topography of the working tool edge.

The obtained results were checked on special equipment with connected electric machines, which has made it possible to check the obtained results when drilling holes in the products made of KIMF material [15].

The drills shown in Fig. 9, b were used for processing until complete damage (Table 3). The stability time  $T$  and parameters of the defects before the onset of the critical drill state were evaluated. We compared the work with cyclic feed and without it. The following was checked during the control:

- presence of damage in the diamond-bearing layer and the relative area of the grain breakdown areas is characterized by the coefficient  $k_{oa}$ ;
- presence of areas of substrate damage,  $k_{sb}$ ;
- presence of a violation of the substrate adhesion to the base  $k_{sp}$ .

The obtained diagrams of influence of the amplitude of oscillation of the working tool surface, diamond grain protrusion, and density of grain distribution on the phenomena of withdrawal of slime particles outside the cutting zone (Fig. 14) are identical to the theoretical theses shown, in particular, in Fig. 7.

In addition, the density of the tool surface contamination with the slime of the processed material was also determined. The material was processed in cycles of 1.0 min with the prevention of dense surface contamination.

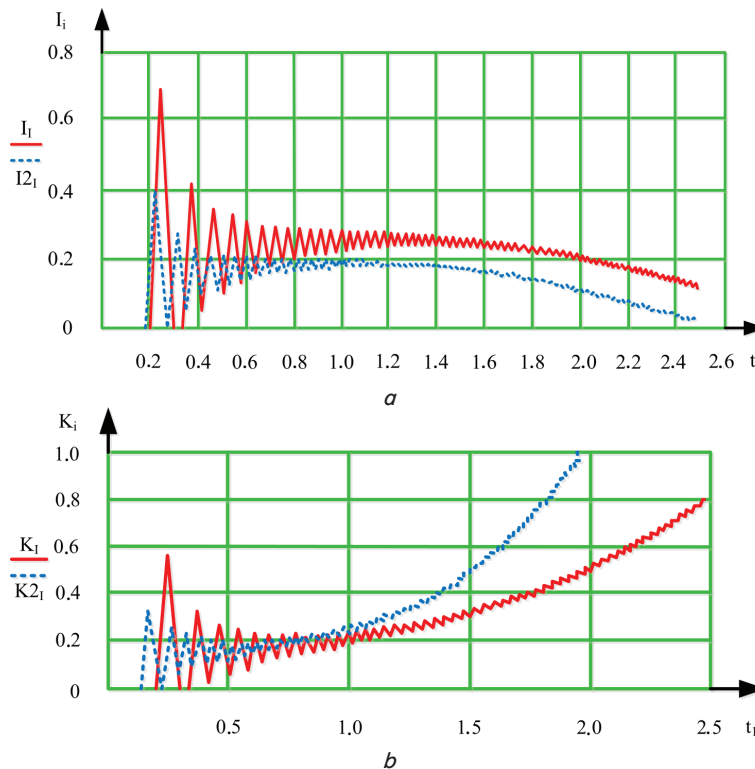
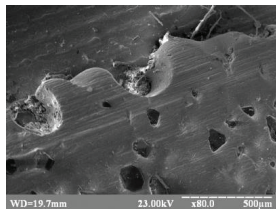
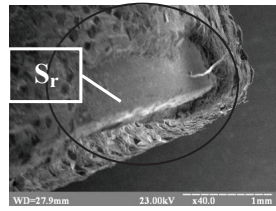
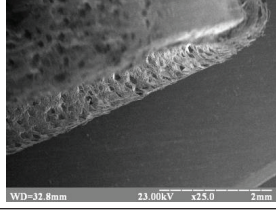


Fig. 13. Simulation of the change in intensity of emission of slime particles in the interfacial gap in the involute on the time axis  $t_1$ : a – by the number of  $l_i$ ; b – by concentration in the gap

Table 3

Typical defects of the ring drills  
(diamond layer thickness: 0.1 mm, grain concentration: 54–62 pcs/cm<sup>2</sup>, grain size: 0.13–0.15 mm)

No.	Defect type	Example	Controlled parameter	Number of defects	
				With continuous advance	With cyclic advance
1	Presence of damage in diamond-bearing layer and relative area of sections with grain break-down		$k_{oa} = \frac{N_a}{N_{cep}} = \frac{22}{58} = 0.379$	2	8
2	Presence of sections with the damaged substrate		$k_{sb} = \frac{S_b}{S_o} = \frac{7}{320} = 0.022$	2	5
3	Presence of dis-bonding between substrate and base		$k_{sp} = \frac{S_p}{S_o} = \frac{18}{320} = 0.056$	1	4

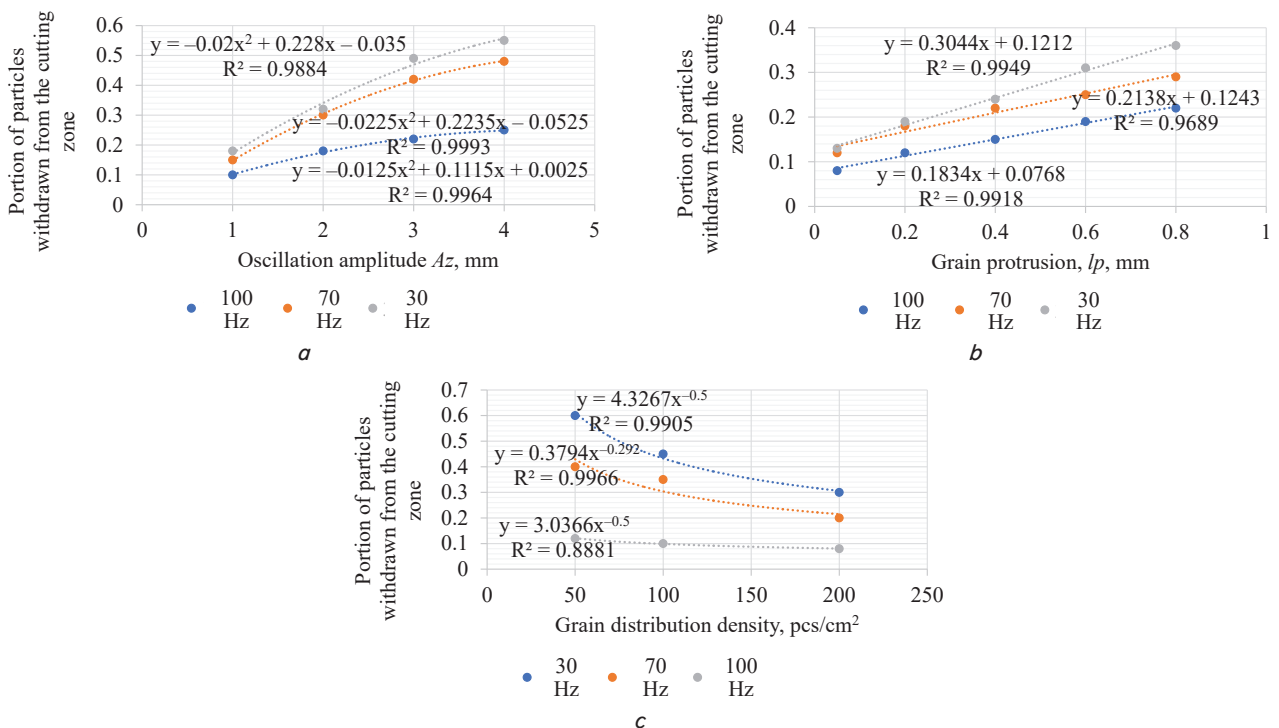


Fig. 14. Influence of individual factors on the phenomena of particle withdrawal outside the cutting zone: *a* – oscillation amplitude (polynomial); *b* – grain protrusion (linear); *c* – density of grain distribution (power)

Comparing the experimentally established contact area with the calculated theoretical area  $s_t$  using the procedure for the case of cutting with conventional tool advance, we obtained the density of contamination of the tool surface  $\psi_b$ ,  $y_k = s_t/\bar{s}$ .

Various tool designs were tested in the study.

The results are presented in Table 4.

Measurements of controlled quantities and calculation of the  $\psi_k$  parameter have allowed us to construct dependence of the latter on the time function (Fig. 15). It is seen that this dependence is satisfactorily described by a linear regression model of this form:  $y = b_0 + b_1x$ .

Table 4

Calculation of the contact area  $s_i$  according to the set parameters  $F_p$  and  $T_i$

No.	Process parameters		$s_i$	$\bar{s}$	$s_t$	$\Psi_k$	$\Psi_k$	$\Psi_k$	$\Psi_k$
	$F_p, N$	$T_i, K$							
New tool: operation time $\tau=5$ min									
1	82	610	96.2	92.23	186.0	0.495	0.458	0.431	0.473
2	84	599	89.3						
3	75	570	92.6						
4	79	575	90.8						
Operation time $\tau=15$ min									
1	101	670	104.2	103.87	186.0	0.558	0.492	0.45	0.512
2	98	660	102.8						
3	95	675	105.3						
4	97	665	103.2						
Operation time $\tau=30$ min									
1	110	702	110.4	110.42	186.0	0.593	0.502	0.501	0.554
2	108	690	108.1						
3	118	700	112.3						
4	121	685	110.9						
Operation time $\tau=45$ min									
1	149	750	116.7	118.8	186.0	0.643	0.525	0.552	0.584
2	146	730	118.5						
3	153	745	119.2						
4	164	732	120.8						

in the efficiency of slime withdrawal should also be expected with an increase in the density of diamond grain distribution.

Fig. 15 also shows the results of studies of the degree of contamination of tools with fundamental differences in the diamond layer such as periodically missing layer (forming 3) and clustered layers (forming 1, forming 2). A conclusion can be drawn from the given diagrams that alternation of clusters of a diamond-bearing layer reduces the phenomenon of sticking of dirt particles to the tool surface. Therefore, the tool stays free of dirt for longer, and processing is thus more efficient.

Thus, the proposed principle of forming an abrasive surface as individual clusters is quite promising as it partially solves the problem of improving the machinability of carbon-based materials by creating rational parameters of the tool surface layer. Further studies should be aimed at determining the effects of adhesion of particles to each other, the formation of slime conglomerates, and the search for effective means to reduce the surface activity of slime.

**6. Discussion of the results obtained in determining the dust impact on the cutting process**

The study of features of the process of abrasive cutting carbon-carbon composites, the phenomena of emission and propagation of slime and dust, fractionality of the latter and determining the factors influencing the efficiency of withdrawal of destruction products from the cutting zone has made it possible not only to solve the practical problem of improving processing efficiency but also clarify certain points regarding the fracture mechanics for this class of materials.

Application of a PSE-based modeling approach combined with consideration of fracture of the material and the workpiece fragments integrally as a quasi-brittle body is an effective tool for describing the interaction of an anisotropic medium with a hard indenter represented by a single diamond grain. This has allowed us to draw a conclusion on the correspondence of the slime particle size to the conditions of growth of cracks before their bifurcation.

Identification of the equation (1) parameters will also indirectly help predict the thickness of the destructible layer, that is, the layer in which cracks were initiated but did not develop to critical dimensions (Fig. 8). No doubt, there are differences in particle size caused by the fact that the fibers can be separated from the pyrocarbon matrix by significant stresses occurring in the cutting zone. However, such differences must be studied further because raster studies of microelectronic photos give reason to believe that number of such particles does not exceed 5%.

Certainly, the considerations expressed relate to the carbon-carbon group of materials belonging to KIMF ma-

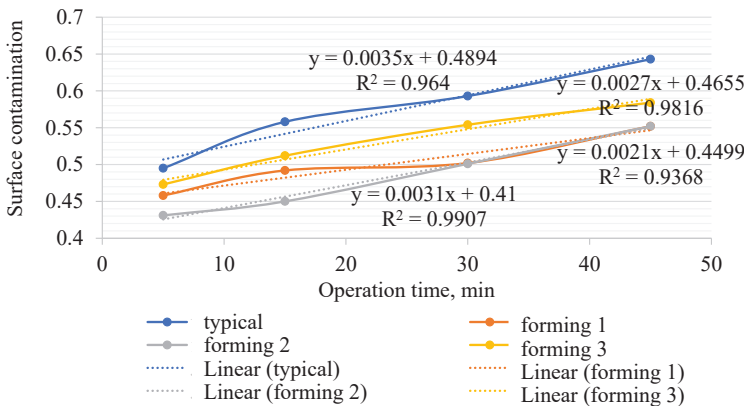


Fig. 15. Variation of the degree of layer surface contamination by the products of destruction during the processing of KIMF material ( $\psi$  parameter) as a function of time

Thus, a regularity of variation of density of surface contamination was established. It was shown that the parameter of relative contamination (equal to the ratio of the contact area of a new tool to the contact area of a tool that has worked for some time) increased almost linearly as a function of time. The increase in contamination leads to an increase in temperature and force load on the contact spot. Under certain conditions, this can cause damage to both the tool and the workpiece. It should be noted that the reduction of grain protrusion above the surface will lead to a reduction in the number of withdrawn particles caused by the reduction of instantaneous slime concentration. A decrease



terials. The behavior of plastics, including those based on carbon fibers, will have some differences, as the binder no longer appears as a quasi-brittle body exhibiting more plastic-elastic properties. Another point that indirectly takes into account the fracture model is the difference in size and location of the material cavities. It should also be noted that the thermal model does not take such features into account at all (10). And again, the difference between the calculated temperature values given in Fig. 10 from the values obtained by pyrometry makes 10–15 % and tends to increase with prolonged cutting.

Because this study has shown that the particle sizes and movement in gaps are conditioned by the temperature at the points of contact of diamond grains with the processed material (Fig. 13). This error causes some discrepancy between the expected degree of damage to the selected tool (ring type drills) in a continuous and reciprocal tool advancement.

However, at the same time, an immediate important conclusion may be the conclusion on the prospects of processing using tools with clusters of a diamond layer, which differ in certain features (for example, alternation of surface sections with multidirectional grains, grains of different fractions and densities of their laying on the surface, with strips without grains, etc.).

For any case, the need to take into account the phenomena of slime emission is appropriate.

Thus, further studies should be aimed at the development of engineering procedures for predicting slime emissions with simple regression equations, designing means to increase the efficiency of slime removal from the cutting zone (and, accordingly, from the tool surface) which will significantly increase the efficiency of KIMF-type materials.

---

## 7. Conclusions

---

1. Regularities of dust emission during the processing of composite carbon-carbon materials were obtained and it was

shown that the intensity of dust emission changes with time getting lower with an increase in the processing time. When using abrasive tools, the size of dust particles is 0.3–0.8 the size of diamond grains. There is a close correlation between the force applied to the tool edges (and, accordingly, the stresses in the cutting zone) and the surface profile parameters: force growth results in a progressive increase in slime particle size caused by the destruction of the cutting layer. A decrease in the height of diamond grain protrusion increases dust dispersity.

2. The effect of dust and slime emission on temperature change in the cutting zone was established. It was shown that the worsening of withdrawal of dust and slime particles from the cutting zone leads to their active sticking to the tool surface which changes cutting properties of the latter resulting in higher contact pressures and surface temperature. For an uncontaminated tool, the temperature at the contact surface tends to reach critical values above 600–700 °C within 2–2.5 min of the tool operation. This requires measures to be taken for a more efficient withdrawal of particles outside the cutting zone.

Carbon slime in a form of pyrocarbon particles and residues of reinforcing fibers must be completely withdrawn from the cutting area as when left on the surface, they will get more compact, cause an increase in the contact area and lead to a fairly active increase in the cutting zone temperature up to 800 °C in 1.5–2 min.

3. Application of a cyclic load (within 30–60 Hz) to the working tool edges makes it possible to partially stabilize the process of dust withdrawal outside the processing area. The use of tools with a cyclic advance partially improves conditions of material processing through the removal of slime particles due to tool oscillations with a low frequency of 30–50 Hz with an amplitude of up to 1–2 mm and prolong time to contamination by an average of 50–80 %.

4. It was proved that intermittent diamond-bearing layer sections reduce the phenomenon of dirt particle sticking to the tool surface. Therefore, the tool stays free of dirt for longer, and processing is thus more efficient.

---

## References

1. Sheikh-Ahmad, J. Y., Davim, J. P. (2012). Cutting and Machining of Polymer Composites. Wiley Encyclopedia of Composites, 2, 648–658. doi: <https://doi.org/10.1002/9781118097298.wec061>
2. Bayraktar, S., Turgut, Y. (2016). Investigation of the cutting forces and surface roughness in milling carbon-fiber-reinforced polymer composite material. *Materiali in Tehnologije*, 50 (4), 591–600. doi: <https://doi.org/10.17222/mit.2015.199>
3. Wang, H., Sun, J., Li, J., Lu, L., Li, N. (2015). Evaluation of cutting force and cutting temperature in milling carbon fiber-reinforced polymer composites. *The International Journal of Advanced Manufacturing Technology*, 82 (9-12), 1517–1525. doi: <https://doi.org/10.1007/s00170-015-7479-2>
4. Venkatesh, B., Singh Sikarwar, R. (2018). Drilling of Carbon Fibre Reinforced Polymer Materials - A Review. *International Journal of Mechanical and Production Engineering Research and Development*, 8 (2), 157–166. doi: <https://doi.org/10.24247/ijmperdapr201817>
5. Geier, N., Davim, J. P., Szalay, T. (2019). Advanced cutting tools and technologies for drilling carbon fibre reinforced polymer (CFRP) composites: A review. *Composites Part A: Applied Science and Manufacturing*, 125, 105552. doi: <https://doi.org/10.1016/j.compositesa.2019.105552>
6. Melentiev, R., Priarone, P. C., Robiglio, M., Settineri, L. (2016). Effects of Tool Geometry and Process Parameters on Delamination in CFRP Drilling: An Overview. *Procedia CIRP*, 45, 31–34. doi: <https://doi.org/10.1016/j.procir.2016.02.255>
7. Pinho, L., Carou, D., Davim, J. (2015). Comparative study of the performance of diamond-coated drills on the delamination in drilling of carbon fiber reinforced plastics: Assessing the influence of the temperature of the drill. *Journal of Composite Materials*, 50 (2), 179–189. doi: <https://doi.org/10.1177/0021998315571973>

8. Ma, F. J., Zhu, X. L., Kang, R. K., Dong, Z. G., Zou, S. Q. (2013). Study on the Subsurface Damages of Glass Fiber Reinforced Composites. *Advanced Materials Research*, 797, 691–695. doi: <https://doi.org/10.4028/www.scientific.net/amr.797.691>
9. Bonnet, C., Poulachon, G., Rech, J., Girard, Y., Costes, J. P. (2015). CFRP drilling: Fundamental study of local feed force and consequences on hole exit damage. *International Journal of Machine Tools and Manufacture*, 94, 57–64. doi: <https://doi.org/10.1016/j.ijmachtools.2015.04.006>
10. Kirichenko, A., Al Ibrahim, M., Schetin, V., Chencheva, O. (2018). Improving the quality of abrasive cutting carbon-carbon composites through rational conditions of dynamic contact. *Transactions of Kremenchuk Mykhailo Ostrohradskyi National University*, 5 (112), 94–102. doi: <https://doi.org/10.30929/1995-0519.2018.5.94-102>
11. Al-wandi Sinan, Ding, S., Mo, J. (2017). An approach to evaluate delamination factor when drilling carbon fiber-reinforced plastics using different drill geometries: experiment and finite element study. *The International Journal of Advanced Manufacturing Technology*, 93 (9-12), 4043–4061. doi: <https://doi.org/10.1007/s00170-017-0880-2>
12. Tsao, C. C., Hocheng, H., Chen, Y. C. (2012). Delamination reduction in drilling composite materials by active backup force. *CIRP Annals*, 61 (1), 91–94. doi: <https://doi.org/10.1016/j.cirp.2012.03.036>
13. Chenchevaya, O., Salenko, A. (2014). About expedience the use of compounds of rotating electrical machines in the power head of new technological equipment. *Transactions of Kremenchuk Mykhailo Ostrohradskyi National University*, 4 (87), 111–118. Available at: [http://visnikkrnu.kdu.edu.ua/statti/2014\\_4\\_111.pdf](http://visnikkrnu.kdu.edu.ua/statti/2014_4_111.pdf)
14. Salenko, A., Chencheva, O., Lashko, E., Shchetynin, V., Klimenko, S., Samusenko, A. et. al. (2018). Forming a defective surface layer when cutting parts made from carbon-carbon and carbon-polymeric composites. *Eastern-European Journal of Enterprise Technologies*, 4 (1 (94)), 61–72. doi: <https://doi.org/10.15587/1729-4061.2018.139556>
15. Kuznietsov, V., Shinkarenko, V. (2011). The genetic approach is the key to innovative synthesis of complicated technical systems. *Journal of the Technical University at Plovdiv, Bulgaria Fundamental Sciences and Applications*, 16, 15–33. Available at: [http://www.tu-plovdiv.bg/Container/journal/journal\\_V16\\_book2.pdf](http://www.tu-plovdiv.bg/Container/journal/journal_V16_book2.pdf)